



1 **Exploration of virtual catchments approach for runoff predictions of** 2 **ungauged catchments**

3 Jun Zhang¹, Dawei Han¹, Yang Song¹, Qiang Dai²

4 ¹Department of Civil Engineering, University of Bristol, Bristol BS8 1TR, UK

5 ²Key Laboratory of VGE of Ministry of Education, Nanjing Normal University, Nanjing, 210000, China

6 *Correspondence to:* Jun Zhang (jun.zhang@bristol.ac.uk, catherine.zjun@gmail.com)

7 *Competing interests.* The authors declare that they have no conflict of interest.

8 **Abstract.** We explore unit hydrograph (UH) properties influenced by catchment geomorphology that could be used in
9 ungauged catchments. Unlike using gauged catchments, a robust approach with virtual catchments was adopted in deriving
10 UH equations. Over 2000 virtual catchments were created from the baseline model of the Brue catchment, UK. A distributed
11 model, SHETRAN, was used to generate runoff in these catchments. Using virtual catchments is feasible to control catchment
12 geomorphologies, which could not be done with the real catchments due to their vast heterogeneity. Catchment characteristics
13 of average slope, drainage length and a new index of catchment shape were examined of their influence on UH properties. The
14 agreement of the results with the hydrological principles is a useful validation of the approach (e.g., the increasing slope led
15 to quick response to peak (T_p) and high peak volume (Q_p) of UH, whereas the drainage length presented an opposite trend).
16 Catchment shape was shown to have a significant effect on UH properties. Compared with the widely used empirical equation
17 from the U.K. Institute of Hydrology, the drawn conclusion recommends more indicators to be included to derive more
18 comprehensive equations: apart from catchment geomorphologic properties, storm patterns including storm intensity and
19 temporal distribution are also influential on the UH shape. The indicators in this study were limited to generate a sophisticated
20 equation for use. However, these results can be considered as a testing case to gain more understanding in hydrologic processes
21 for ungauged catchments with the help of the virtual catchment approach.

22 **1 Introduction**

23 Runoff modeling in ungauged catchments needs a large quantity of data for purposes of generalization. Our knowledge of
24 catchment responses is not adequate to simply transfer models derived from a gauged to an ungauged catchment (Sivapalan,
25 2003). The heterogeneity of catchment geomorphology, e.g. its terrain, area, shape, land surface condition, soil types, etc., is
26 the root cause of the difficulty in predicting catchment response (Hrachowitz et al., 2013; Pilgrim et al., 1982; Sivapalan, 2003).
27 Transferring model parameters from one catchment to another is linked to regional catchment characteristics (Bárdossy, 2006;
28 Castiglioni et al., 2010; Young, 2006) as the dominant control on runoff production and routing (Beven et al., 1988; Beven
29 and Wood, 1983). Therefore, understanding the catchment geomorphological impact on runoff is crucial to predicting
30 streamflow in ungauged catchments. Among all hydrological approaches, the unit hydrograph (UH) is recognized as being an
31 effective prediction tool and is deemed to reflect the characteristics of the catchment with the potential to estimate the
32 streamflow in ungauged catchments (Sherman, 1932).

33 Hydrologists have been attempting to derive UHs from catchment descriptors for decades. The possibility to extract UHs from
34 catchment characteristics was proposed by Bernard (1935), followed by the early synthetic UH development strategies (Snyder,
35 1938; Taylor and Schwarz, 1952), most of which are empirical methods. Further examples of empirical methods can be seen
36 in U.S. Soil Conservation Service (Mockus, 1957) and Singh (1988). The U.K. Institute of Hydrology offered an empirical
37 UH that used 1822 individual rainfall runoff events and 204 catchments in the country (Robson and Reed, 1999). Catchment
38 area, drainage length, distance to the outlet, land use, antecedent soil condition etc., are considered in these methods. Most



39 traditional UH methods establish a set of empirical relations among catchment characteristics to describe the shape of UH on
40 the basis of gauged catchments, which have certain region-specific constants/coefficients varying over a wide range (Singh et
41 al., 2014). Its inconsistency due to subjectivity and manual fitting makes it a challenge to apply in ungauged catchments or
42 different regions. Moreover, another main obstacle is how to choose catchment data sets properly. Either small data sets or
43 catchments with widely varying characteristics hamper the derivation of a UH that can be used to represent the ungauged
44 catchments (Van Esse et al., 2013; Robinson et al., 1995).

45 Apart from empirical methods, conceptual models represent a catchment as a series of linear storages and are based on
46 continuity equations and the storage discharge (Clark, 1945; Nash, 1957). This simplification ignores the flow translation in
47 the catchment, which is essential to describe the behavior of a dynamic system. What is more, the coefficients are difficult to
48 determine for ungauged catchments; for example, some parameters should ideally be an integer rather than a fractional value
49 derived from catchment characteristics (Singh et al., 2014). With the increasing availability of geographic information system
50 (GIS) data, GIS-supported UH approaches are explored by Jain et al. (2000), Jain and Sinha (2003), Sahoo et al. (2006), and
51 Kumar et al. (2007). These approaches are based upon conceptual UH models to evaluate model parameters related to
52 geomorphological characteristics from GIS packages. However, this improvement of modeling performance does not solve
53 the problems brought by conceptual simplification of the models.

54 Explicitly integrating catchment geomorphology details in the framework of travel time distribution to define a
55 geomorphological instantaneous unit hydrograph (GIUH) is pioneering work that is appeared to be promising in ungauged
56 catchment modeling (Rodríguez-Iturbe and Valdes, 1979; Rodríguez-Iturbe et al., 1982; Valdés et al., 1979). The model
57 properties assessed are highly dependent on geomorphologic elements (Chutha and Dooge, 1990). The GIUH model has
58 generated a wealth of research since its conception. However, it has been criticized because of its assumption of exponential
59 distribution of drainage time mechanism by Gupta and Waymire (1983), Kirshen and Bras (1983), and Rinaldo et al., (1991),
60 and the assumption of uniform celerity of flow has been shown to actually change from storm to storm (Pilgrim, 1977).
61 Moreover, GIUH is not sensitive to rainfall spatial distribution due to the averaging scheme used in the model (Corradini and
62 Singh, 1985). Further, ignoring the effect of catchment slope is unreasonable especially in because small catchments, which
63 are sensitive to hillslope response (Botter and Rinaldo, 2003; D'Odorico and Rigon, 2003; Robinson et al., 1995).

64 The width function-based GIUH (WFIUH) model employed by Rinaldo et al. (1995) shows a better capability to model
65 different transport processes within channeled and hillslope regions. WFIUH has been further improved by Grimaldi et al.
66 (2010, 2012) with spatially distributed flow velocity within a digital elevation model (DEM)-based algorithm. Nevertheless,
67 there are still practical limitations in extracting the network widths especially for large catchments (Sahoo et al., 2006). The
68 freezing parameters for the whole catchment limit the variability of the hydrological scheme (Rigon et al., 2016).

69 Previous studies have put great effort into looking for a general rational formulation linking UH properties with catchment
70 geomorphology. However, due to the limitation of data availability and conceptual simplification of hydrological processes,
71 the lack of understanding of physical principles hinders parameter transferring from gauged to ungauged catchments. To
72 overcome the aforementioned issues, we present a series of virtual catchments to explore streamflow generation in ungauged
73 catchments. Each virtual catchment is assigned particular catchment characteristics including three main indicators i.e., average
74 slope and drainage length, and catchment shape, which are rarely accounted in previous studies. The experiments are
75 undertaken using a fully distributed model, *Système Hydrologique Européen TRANsport*(SHETRAN), for simulating the
76 catchment response, the results of which are compared with the standard UH equations in the widely used Flood Estimation
77 Handbook (FEH) proposed by the U.K. Institute of Hydrology in UK (Robson and Reed, 1999).



78 2 Methodology and data sources

79 2.1 SHETRAN

80 SHETRAN is a physically based spatially distributed hydrological model for water flow and sediment and solute transports in
 81 catchments (Ewen et al., 2000), which is originated from the Système Hydrologique Européen (SHE) (Abbott et al., 1986).
 82 SHETRAN provides an integrated representation of water movements through a catchment, containing major elements of the
 83 hydrological cycle as shown in Table 1. It models streamflow in a single complete river catchment by retrieving data for a
 84 catchment, including weather data, river gauge recordings, catchment properties, e.g. DEM, land use and soil type. The
 85 catchment is represented by an orthogonal grid, which allows spatial distribution of input data, including rainfall, meteorological
 86 data and catchment properties, etc. The model has been applied in varied catchments and has proved to be a reliable
 87 hydrological model (Birkinshaw and Ewen, 2000; Hipt et al., 2017; Norouzi Banis et al., 2004; Zhang et al., 2013).

88 2.2 Flood Estimation Handbook prediction

89 An empirical equation of instantaneous unit hydrograph (IUH) derived from regression analysis with 1822 individual events
 90 and 204 catchments has been proposed by the U.K. Institute of Hydrology and has been widely adopted in practical streamflow
 91 prediction; it is referred to the FEH equation in this study (Robson and Reed, 1999). Four catchment descriptors are used to
 92 predict the time to peak (T_p) in IUH as shown in Equation (1).

$$93 \quad T_p = 4.270 S^{-0.35} W^{-0.80} L^{0.54} (1 - U)^{-5.77} \quad (1)$$

94 in which, T_p is the time to peak, in h; S is the mean drainage path slope (m km^{-1}); W is the proportion of time when soil
 95 moisture deficit is below 6mm (%); L is an index describing drainage path (km); U is the extent of urban and suburban land
 96 cover (km^2).

97 At each grid node, an outflow direction is defined to one of its eight neighboring nodes. Using the difference in altitude and
 98 the distance between the two nodes, the internode slope is calculated. The procedure is repeated for all nodal pairs within the
 99 catchment to give the mean drainage path slope S . Using the drainage paths, the distance between each node and the catchment
 100 outlet along the flow path is calculated; L is the mean value of all these distances. To compare the results from virtual
 101 catchments with the FEH equation, the same methodologies are applied in the following analysis when referring to the same
 102 factors.

103 In the FEH equation, the IUH peak volume Qp is derived from T_p as a regression result and a continuity constraint as shown
 104 in Equation (2)(Robson and Reed, 1999).

$$105 \quad Qp = \frac{2.2}{T_p} \quad (2)$$

106 in which, Qp is the peak volume of UH (mm).

107 In practice, using an optimal interval UH gives a much smoother response. Therefore, it is customary to use convenient
 108 values such as 0.25, 0.5 or 1 h in UH, which can be done with Equation (3)(Robson and Reed, 1999).

$$109 \quad T_p(\Delta t) = T_p(0) + \frac{\Delta t}{2} \quad (3)$$

110 2.3 Study area

111 This study explores the rainfall-runoff behavior embedded with changing catchment geomorphology in the Brue catchment,
 112 UK. The Brue catchment has been a focus of research because of the abundant available data (Dai and Han, 2014; Dai et al.,
 113 2014, 2015; Younger et al., 2009). The Brue catchment comprises 137 km^2 of the river's headwaters and drains to the river
 114 gauge in Lovington (Moore et al., 2000). Figure 1 presents the general spatial characteristics of the catchment in a 500m size
 115 grid that is used in the following analysis. The elevation varies from 251 m in the northeast to 22 m in the southwest. There



116 are three soil types, i.e. mud, clay and sand, with their distribution shown in Fig. 1 according to the national soil type data
117 downloaded from Digimap Service (Soil Parent Material Model, 2011). The slope ranges from 10.85% to 0.07% (transferred
118 to m km^{-1} for further analysis) and shares a similar spatial patterns with the elevation. Flow length mainly depends on the
119 distance from the node to the outlet, ranging from 0 up to 19.81 km.

120 Prior to the execution of the virtual catchments, a baseline distributed model of the Brue catchment was configured and then
121 calibrated and validated with historical measured data in the Brue catchment. The calibration was based on the hourly data in
122 1995 and validation with the hourly data in 1996 involved the collection of discharge and meteorological data. We used the
123 streamflow at the outlet for model calibration and validation. The baseline model of the Brue catchment was constructed from
124 a 50 m DEM with the grid cell size of 500 m. The stream network was derived automatically from the DEM in the model. The
125 average slope of the catchment is 29.18 m km^{-1} and the average drainage length is 12.12 km.

126 The catchment was schematized as an orthogonal grid in SHETRAN integrated with a spatially variable geomorphology. To
127 examine the runoff response to variable catchment characteristics, change of catchment geomorphologies (mainly on the role
128 of average slope, drainage length and catchment shape) were specified in a large number of virtual catchments. When verifying
129 one element, the other geomorphological features were kept unchanged. A UH was generated from each simulation to evaluate
130 the relationship between UH and catchment properties, which were eventually used in ungauged catchments. During the
131 experiment, although some of the virtual catchments were extreme when compared with the real catchment conditions, they
132 still allowed the useful insights to be gained in understanding the role of catchment geomorphology on runoff generation.

133 3 Results

134 3.1 Model validation

135 With the real soil map information, we used experimental soil parameters by the Boreal Ecosystem-Atmosphere Study Data
136 Sets hydrology (BOREAS HYD-01) team (Kelly and Cuenca, 1998). However, due to a lack of land use data in the catchment,
137 a homogeneous land use map was assigned in the model with calibrated land use parameters. The model was evaluated with
138 Nash-Sutcliffe efficiency (NSE) (Nash and Sutcliffe, 1970), which is generally adopted in hydrological research (Guerrero et
139 al., 2013; Parasuraman and Elshorbagy, 2008; Rojas-Serna et al., 2016; Zhuo et al., 2015).

140 In previous hydrological modeling, the simulation of discharge is commonly acceptable when NSE is greater than 0.8 (Beven
141 and Binley, 1992; Freer et al., 1996). In this study, the calibrated NSE was 0.82 and the validated NSE 0.81 with the hydrograph
142 shown in Fig. 2. Due to the calculation function of NSE, it is more sensitive to higher flow than lower values so the analysis
143 is very useful in peak flow studies, as shown in Fig. 2 (Krause et al., 2005). There are numerous rainfall events in both dry and
144 wet seasons of one year in the Brue catchment, therefore, the model is fully excited with abundant information. The qualified
145 performance demonstrates that SHETRAN is capable of providing a realistic representation of the catchment hydrology in the
146 case site.

147 3.2 Average slope

148 Response of streamflow on the average slope was examined by changing the elevations across the catchment on the basis of
149 the original topography. All the grids were multiplied by the same factor varying from 0.2 to 4 in individual virtual catchments
150 so that the average slope changes from 5.84 m km^{-1} to 116.72 m km^{-1} . In the meantime, other properties such as catchment
151 area and grid size remained unchanged to avoid compounding effects. A uniformly distributed rainfall of 10 mm for 1 h was
152 applied for simulating outlet runoff in SHETRAN.

153 With the slope varying from 5.84 m km^{-1} to 116.72 m km^{-1} , T_p in the UH decreased from 17 to 7 h with a clear power
154 declination displayed in Fig. 3 (Kirpich, 1940; Robson and Reed, 1999). Since the catchment is relatively small, the runoff



155 generation is not quite sensitive in the hourly time step, which presents the same values among similar slopes, e.g. the slope
156 group from 70 m km⁻¹ to 116.72 m km⁻¹.

157 By testing several trend lines with the results and based on the reference of FEH equations, a power function is used in this
158 study to describe the trend. A standard form of power function $y = ax^b$ was integrated with two coefficients a and b . To
159 distinguish from the other coefficients, the above were labelled a_1 and b_1 in this experiment and specific subscripts are used
160 respectively for the following results. Compared to the FEH equation stated in Equation (1) with the relationship of average
161 slope, b_1 was -0.35 while b_1 was -0.29 displayed in Fig. 3. When the absolute value b_1 was smaller, a less significant
162 relationship was found between the two variables.

163 3.3 Drainage length

164 3.3.1 Drainage length and average slope

165 The same uniform rainfall as the previous experiment was distributed for the experiment on the effect of drainage length (L)
166 on runoff response. The catchment cell size was multiplied by certain factors ranging from 0.1 to 10, leading to values of L
167 from 1.21 km to 121.20 km. Nine different groups of virtual catchments were generated with different slope values for further
168 analysis, ranging from 14.59 to 116.72 m km⁻¹. To maintain the average slope of these virtual catchments unchanged in each
169 group, the elevation values in each catchment were also changed by multiplying them by the same factor. In Fig. 4, five of the
170 nine groups are marked in the legend with the multiple factor of the slope, e.g., 'slope 0.5' means the average slope of this
171 groups is 14.59 m km⁻¹. The derived equations are listed in Table 2 with a_2 and b_2 for the nine groups.

172 All groups demonstrated a similar trend in which the longer L is, more time it needed to reach the peak volume of UH, which
173 presents a power function as well. Moreover, when the streamflow drained the same length with different slopes, it took a
174 shorter time to reach the outlet on steeper catchments, which is consistent with the result in the previous sections and other
175 studies (Kirpich, 1940; Robson and Reed, 1999).

176 As seen in Table 2, a_2 decreased from 0.94 to 0.53 when the slope increased from 14.59 to 116.72 m km⁻¹. Meanwhile, b_2
177 experienced a slight fluctuant around 1.10. The coefficient a_2 is best represented at the starting point of the line, while larger
178 a_2 indicated a longer Tp when the catchment is small and flat. Referring to the derived equations, both a_2 and b_2 decrease in
179 steeper catchments. Values of b_2 are greater than that adopted in the FEH equation (0.54), which presents a greater rate of
180 increase of the trend. The results demonstrate that Tp from the catchments in the experiments are more sensitive to L than in
181 the FEH equation. Moreover, b_2 experienced an increase with the increase of slope followed by a decrease, which implies that
182 L is of more importance when the catchment is steeper. However, the significance of L was weaker when the steepness kept
183 increasing.

184 3.3.2 Drainage length and storm patterns

185 The experiments on changing slope and L showed similar trends with the FEH equation. However, the coefficients were vastly
186 different. In the previous experiments, a homogenous rainfall with 10 mm in 1 h was applied, which is not realistic for real
187 catchments and also different from the storms chosen to derive the FEH equation. It is also shown that UHs from varied storms
188 can be different (Corradini and Singh, 1985; Rigon et al., 2016; Valdés et al., 1979). Thus, to further explore the UH generation
189 from storms with different intensities and durations, multiple rainfall events were applied to the virtual catchments.

190 S , W and U were held constant at the original value of the catchment and only L was changed in this experiment. FEH was
191 derived by replacing W and U with the real data and eventually presented by a function with an independent variable L .

192 The relationship between Tp and L derived from varied storms is shown in Fig. 5 and Table 2 with coefficients of a_3 and b_3 .
193 Table 2 presents a full list of experiments with examples of experiments shown in Fig. 5. In Fig. 5 (a), rainfall is uniformly
194 distributed in the catchment with varied intensities (from 10 mm to 80 mm) for 1 h. A clear trend was seen in each storm



195 between T_p and L , while for larger storms both a_3 and b_3 decreased, as seen in Table 2. T_p appears to decrease for larger
196 storms in both small and large catchments. Moreover, the difference between small and large catchment becomes smaller when
197 the storm intensity increases. The larger a_3 in the FEH equation was overestimated in small catchments while the smaller b_3
198 illustrates that underestimated L influences discharge predictions for large catchments.
199 More patterns are presented in Fig. 5 (b) when storms with different durations of the same rainfall intensities (10 mm h^{-1}) were
200 explored. When the duration increased, a_3 presented an increasing trend while b_3 showed an opposite trend. Similar to what
201 was seen in Fig. 5 (a), large storms were less sensitive to catchment size with decreasing b_3 . However, increasing a_3 illustrates
202 that small catchments took longer to reach the peak volume when the storm duration increased. For catchments with longer
203 drainage length, there was a lower effect of storm duration on runoff generation, which also exhibited a declining trend.
204 More comparisons were carried out between different temporal distributions of rainfall on runoff generation as shown in Fig.
205 6 and Table 2. Figure 6 (a) presents T_p derived from 10 mm, 20 mm and 50 mm in varied durations. For the storms of 20 mm
206 in two temporal patterns, T_p showed little difference with similar values between coefficients of a and b . However, the storm
207 of 50 mm displayed a more apparent trend of T_p , with L in two patterns. Larger discrepancies can be found in Fig. 6 (b), which
208 depicts that the storms of 100 mm and 200 mm were more sensitive on temporal patterns. The value of a increases when storm
209 duration is lengthened while b experienced an opposite trend. When storm duration was longer, it took longer to reach the
210 peak volume in small catchments. However, if the drainage length was long enough compared to the storm duration, the
211 influence of storm duration decreased, which is clearly shown in Fig. 6 (a) for the 50 mm storm with an intersection of two
212 lines. A longer storm required a longer L to eliminate the impact of rainfall duration, as displayed in the lines for 100 mm and
213 200 mm in Fig. 6 (b).

214 3.4 Catchment shape

215 Catchment shape is not among the factors included in the FEH equation as well as other research on catchment geomorphology.
216 A simple experiment with three catchments of different shapes was carried out in this study as shown in Fig. 7 with the general
217 information in Table 3. Catchment A is the original Brue catchment, and the other two catchments are its transformed clones.
218 Catchment B was transformed by extending the catchment in the north-south direction and shortening in the east-west direction
219 of the original catchment, while Catchment C is in the other way around, i.e., lengthened E-W and shortened N-S. Owing to
220 the symmetry of the original catchment, the generated catchments all had a close resemblance in areas, drainage lengths and
221 slope. All catchments are represented with the same cell size of 500 m. A homogenous rainfall of 10 mm with 1 h duration
222 was applied to the three catchments and then the corresponding UHs from varied L was evaluated.
223 Figure 8 and Table 2 with coefficients of a_4 and b_4 illustrate the relationship between T_p and L in the three different shapes.
224 Figure 8(b) is a zoomed-in view of a portion of Fig. 8(a) when L is smaller than 20 km. T_p varied in the catchments with
225 different shapes even with similar catchment descriptors. With all the other characteristics controlled, the shape of Catchment
226 C presented the longest drainage time. Catchment A experienced the quickest drainage time when L was greater than 20 km,
227 and Catchment B was the fastest when L was shorter than 20 km. Focusing on the scatter dots when L is greater than 100 km
228 in Fig. 8 (a), it is found that T_p from Catchment B and C were close and T_p from Catchment A remained smaller than from B
229 and C. Moreover, the smallest coefficient in the equation b_4 of Catchment A demonstrates that the original shape was the least
230 sensitive to the change of L .

231 3.5 Relationship between Q_p and T_p

232 The analysis between Q_p and L in terms of different slopes and shapes is displayed in Fig. 9 and Table 4 with the coefficients
233 of a_5 and b_5 . A power decreasing relationship was also recognized in Fig. 9 for all the experiments, which is also demonstrated
234 in previous studies (Rinaldo and Rodríguez-iturbe, 1996; Rodríguez-Iturbe and Valdes, 1979). The increased slope results in
235 higher peak volume while coefficient a_5 in the power function was more sensitive to slope than b_5 in Fig. 9(a). This means



236 that the effect of slope and drainage length is more significant for small catchments than for large ones. Moreover, Catchment
237 C presented the highest peak volume while Catchment B experiences the lowest peak volume as shown in Fig. 9(b).
238 It is acknowledged from Eq. (2) of the FEH equation that Qp is inversely proportional to Tp with a coefficient of 2.2 for all
239 the catchments. Similar results can be found in previous studies with different coefficients (Moussa, 2003; Rinaldo and
240 Rodriguez-iturbe, 1996). Taking $y = c/x$ as a representation of the inversely proportional function with c as the main
241 coefficient, Qp from some previous experiments are plotted against Tp as shown in Fig. 9(c)-(d), with the equations shown in
242 Table 4. Obviously, an inversely proportional relationship was clearly shown between Qp and Tp for all the experiments.
243 However, c was not consistent for varied storms in catchments with different geomorphologies. Figure 9(c) and (e) exhibit Qp
244 from storms with varied intensities and temporal distributions. From Fig. 9(c) it can be found that c decreases with longer
245 storm duration and Fig. 9(e) showed that c increased with larger storm intensities. Figure 9(d) demonstrates that catchment
246 slope had little influence on the relationship between Qp and Tp . What is more, catchment shape is also influential on how to
247 deduce Qp from Tp in UH. The value of c was largest in Catchment C while smallest in Catchment A. Therefore, this may
248 result in errors when applying a uniform equation to obtain Qp from Tp in the UH. It is therefore highly recommended to
249 derive various equations based on the catchment geomorphology as well as storm patterns for prediction in ungauged
250 catchments.

251 4 Discussion

252 4.1 The implementation of virtual catchments

253 When transferring knowledge from gauged to ungauged catchments, obstacles exist due to the varied geomorphology and
254 storm types between catchments. Data scarcity also hinders the development of a uniformly acceptable approach for ungauged
255 catchments (Hrachowitz et al., 2013). A common shortcoming of previous empirical UH derivation is that the catchments used
256 are extremely diverse (Corradini and Singh, 1985; Robson et al., 1995; Robson and Reed, 1999; Sawicz et al., 2014; Valdés
257 et al., 1979). For instance, it is hard to control other characteristics (e.g., drainage length, shape, soil, etc.) when we try to
258 investigate how a single catchment element (such as average slope) affects the unit hydrograph. It is already pointed out that
259 error exists with the coefficient of determination $r^2 = 0.74$ from the FEH-derived equation (Robson and Reed, 1999).
260 Moreover, the existing conceptual UH models are mostly based on Horton ratios or other river disciplines (Chutha and Dooge,
261 1990; Gupta et al., 1980; Rodríguez-Iturbe and Valdes, 1979), which are prone to ignore some catchment features. Peña et al.
262 (1999) found that there was not a unique hydrograph for distinct watersheds with similar Horton ratios.

263 In this study, we have used a virtual experiment approach to seek new understanding of the impacts of catchment
264 geomorphology on runoff generation. Our baseline catchment is the well-studied Brue catchment, using the widely-used model
265 SHETRAN, which has been demonstrated to simulate runoff realistically. Using a fully distributed model, we performed a set
266 of model experiments to simulate the streamflow in thousands of virtual catchments. The experiments explored how catchment
267 geomorphology could influence the runoff generation in terms of UH properties, which is informative in ungauged catchments.
268 The advantage of virtual catchments is their simplicity, avoiding unnecessary compounding interferences by controlling of
269 catchment geomorphology by defining catchments with desired features. As many catchments as required can be created in
270 this way, solving the problem of data scarcity. With a reliable distributed hydrological model and synthetic rainfall input, the
271 corresponding streamflow is generated without the required measurements. However, extreme catchments are possible,
272 inducing unusual streamflow and potential modeling error. It is worthwhile to consider the boundary conditions carefully when
273 creating catchments. Besides studies of catchment geomorphology, other spatial variability, such as rainfall input, parameter
274 heterogeneity can also be carried out in virtual catchments. More comprehensive results of runoff generation can be obtained
275 with the help of the virtual catchment approach, which can provide further useful information for ungauged catchments.



276 4.2 UH properties from different catchment geomorphologies

277 As widely applied in ungauged catchments, T_p and Q_p are the most important properties to determine UH shape. Average
278 slope, drainage length, catchment shape and storm properties were examined in this study. The slope and drainage length were
279 generally considered in the previous studies but not catchment shape. As acknowledged, nearly all catchment shapes are
280 irregular and it is impossible to have two catchments with the same shape in the real world. Therefore, we explored the effect
281 of catchment shape on runoff generation by virtual catchments. Moreover, we compared the relationship between catchment
282 characteristics with T_p and Q_p with the FEH equation.

283 4.2.1 T_p from different catchment geomorphologies

284 Similar to previous studies, the increase of average slope and drainage area both prolonged the time of flow to reach peak
285 volume with a clear power relationship (Beven and Wood, 1983; Robinson et al., 1995; Robson and Reed, 1999). As noted
286 above, few studies have been done with the regard to the catchment shape. A simple comparison was conducted with three
287 catchment shapes. The results illustrate that the catchment shape was of importance on UH derivation even with similar areas,
288 drainage lengths and average slopes, not to mention the methodologies that used Horton Law to represent the catchment
289 (Chutha and Dooge, 1990; Rodríguez-Iturbe and Valdes, 1979), which defines the catchment morphology with limited
290 indicators. An indicator could be proposed to describe the catchment shape like slope to describe the elevation of the catchment,
291 e.g. the ratio between the distance from the outlet to the farthest node and the longest orthogonal distance. However,
292 quantification of catchment shape requires further investigation.

293 Nevertheless, compared with a uniform equation applying to all catchments with all storms in the FEH equation, it was found
294 that storm patterns also have an effect on UH generation, which is supported by some previous studies (Corradini and Singh,
295 1985; Rigon et al., 2016; Valdés et al., 1979). Not only storm intensity but also temporal patterns were crucial for UH derivation.
296 The catchments with longer drainage length are less likely to be influenced by storm duration if the drainage time is greater
297 than storm duration. Moreover, when storm intensity increased with a fixed duration, T_p decreased regardless of how long the
298 drainage was. Deriving possible UHs from the virtual catchments should be more reasonable than simply transferring
299 parameters from gauged to ungauged catchments. More rainfall patterns both in temporal and spatial scales should be
300 investigated for a more complete understanding.

301 4.2.2 Q_p from different catchment geomorphologies

302 According to the results obtained in the current phase, it has been stated that slope, drainage length and catchment shape all
303 affect peak volume in UH. An inversely proportional relationship is found between Q_p and T_p in these results as well as in
304 the FEH approach. Similar to T_p , it uses a uniform equation for all catchments and storms in the FEH method. Differences are
305 found in the relationship between Q_p and T_p with varied storms and catchment properties. The storm temporal patterns rather
306 than storm intensity were more significant to this relationship. Moreover, the average slope was less important than the
307 catchment shape, but both were much less crucial than the storm distribution. Therefore, it is beneficial to consider storm
308 patterns in deriving Q_p from T_p rather than using a uniform equation in FEH.

309 Overall, increased steepness led to shorter time to peak as well as higher peak volumes, while longer drainage length prolonged
310 the time to peak and brought down the peak volume. Catchment shape, as a new indicator in this study, was also demonstrated
311 to have an influence on UH properties. Moreover, UH was different from storm to storm with varied temporal distribution and
312 rainfall intensities. Therefore, only applying a general UH equation to all catchments and storms does not comprehensively
313 provide precise streamflow prediction in ungauged sites. As a promising and simple approach to be applied in ungauged
314 catchments, UH is worthy of further exploration on how to determine its accurate shape. The virtual catchment approach is a
315 potentially effective method for systematic investigation without the requirement of a large number of gauged catchments.



316 5 Conclusions

317 UH is widely used in ungauged catchment studies, by deducing equations from gauged catchments. However, it ignores the
318 discrepancy existing between the known with the unknown catchments when transferring parameters. The virtual catchment
319 experiments described here generate a series of relationship between catchment geomorphology and UH properties. Average
320 slope, drainage length and catchment shape (as a new indicator) were shown to be influential on UH properties. Moreover, the
321 UH shape differed from storm to storm caused by the storm duration and intensity. Although Qp has an inversely proportional
322 relationship with Tp as mentioned in the FEH equation, catchment characteristics especially for storm patterns are also crucial
323 to the coefficient used in deducing Qp from Tp .

324 These experiments support the findings in previous studies, and have revealed more catchment characteristics that are
325 influential on runoff generation. In spite of the simplicity of deriving a universal single-UH equation for all catchments and
326 storms, it is feasible to apply a more specific UH to an ungauged catchment considering its geomorphology and the storm
327 characteristics with the help of improved computation technology. More importantly, owing to the virtual catchment approach,
328 a huge number of catchments can be created with desirable features to explore how catchment geomorphology would affect
329 runoff generation. This research suggests an alternative for studying the hydrologic processes in ungauged catchments,
330 especially for regions with data scarcity. However, this study should be regarded as a starting point in obtaining more
331 understanding in hydrologic processes with the help of virtual catchments, and we hope it will encourage more studies in this
332 field to improve the proposed methodology to a higher level.

333 6 Data availability

334 The atmospheric data and runoff data in the Brue catchment in this study are freely available on the British Atmospheric Data
335 Centre website (<https://badc.nerc.ac.uk/home/index.html>). The DEM data is freely available on the Digimap website
336 (<http://digimap.edina.ac.uk/>). The Soil Hydraulic Properties. Data set is freely available online (<http://www.daac.ornl.gov>)
337 from Oak Ridge National Laboratory Distributed Active Archive Center.

338 7 Acknowledgement

339 The first author would like to thank the University of Bristol and China Scholarship Council for providing the necessary
340 support and funding for this research. The author Qiang Dai was supported by the National Natural Science Foundation of
341 China (Grant No. 41501429). The authors acknowledge the Dr. Stephen Birkinshaw for the help with SHETRAN in this study.

342 8 Reference

343 Abbott, M. B., Bathurst, J. C., Cunge, J. A., O'connell, P. E. and Rasmussen, J.: An introduction to the European
344 Hydrological System—Systeme Hydrologique Europeen, “SHE”, 2: Structure of a physically-based, distributed
345 modelling system, *J. Hydrol.*, 87(1-2), 61–77, 1986.

346 Bárdossy, a.: Calibration of hydrological model parameters for ungauged catchments, *Hydrol. Earth Syst. Sci.*
347 *Discuss.*, 3(3), 1105–1124, doi:10.5194/hessd-3-1105-2006, 2006.

348 Bernard, M. M.: An approach to determinate stream flow, *Trans. Am. Soc. Civ. Eng.*, 100(1), 347–362, 1935.

349 Beven, K. and Binley, A.: The future of distributed models: model calibration and uncertainty prediction, *Hydrol.*
350 *Process.*, 6(3), 279–298, 1992.



- 351 Beven, K. and Wood, E. F.: Catchment geomorphology and the dynamics of runoff contributing areas, *J. Hydrol.*,
352 65(1-3), 139–158, doi:10.1016/0022-1694(83)90214-7, 1983.
- 353 Beven, K. J., Wood, E. F. and Sivapalan, M.: On hydrological heterogeneity — Catchment morphology and
354 catchment response, *J. Hydrol.*, 100(1-3), 353–375, doi:10.1016/0022-1694(88)90192-8, 1988.
- 355 Birkinshaw, S. J. and Ewen, J.: Nitrogen transformation component for SHETRAN catchment nitrate transport
356 modelling, *J. Hydrol.*, 230(1), 1–17, 2000.
- 357 Botter, G. and Rinaldo, A.: Scale effect on geomorphologic and kinematic dispersion, *Water Resour. Res.*,
358 39(10), 1–10, doi:10.1029/2003WR002154, 2003.
- 359 Castiglioni, S., Lombardi, L., Toth, E., Castellarin, A. and Montanari, A.: Calibration of rainfall-runoff models in
360 ungauged basins: A regional maximum likelihood approach, *Adv. Water Resour.*, 33(10), 1235–1242, 2010.
- 361 Chutha, P. and Dooge, J. C. I.: The shape parameters of the geomorphologic unit hydrograph, *J. Hydrol.*, 117,
362 81–97, 1990.
- 363 Clark, C. O.: Storage and the unit hydrograph, in *Proceedings of the American Society of Civil Engineers*, vol.
364 69, pp. 1333–1360, ASCE., 1945.
- 365 Corradini, C. and Singh, V. P.: Effect of spatial variability of effective rainfall on direct runoff by a
366 geomorphologic approach, *J. Hydrol.*, 81, 27–43, 1985.
- 367 D’Odorico, P. and Rigon, R.: Hillslope and channel contributions to the hydrologic response, *Water Resour. Res.*,
368 39(5), n/a–n/a, doi:10.1029/2002WR001708, 2003.
- 369 Dai, Q. and Han, D.: Exploration of discrepancy between radar and gauge rainfall surfaces driven by the
370 downscaled wind field, *Water Resour. Res.*, 50, 8571–8588, doi:10.1002/2013WR014979.Reply, 2014.
- 371 Dai, Q., Han, D., Rico-Ramirez, M. and Srivastava, P. K.: Multivariate distributed ensemble generator: A new
372 scheme for ensemble radar precipitation estimation over temperate maritime climate, *J. Hydrol.*, 511, 17–27,
373 doi:10.1016/j.jhydrol.2014.01.016, 2014.
- 374 Dai, Q., Han, D., Rico-Ramirez, M. a., Zhuo, L., Nanding, N. and Islam, T.: Radar rainfall uncertainty modelling
375 influenced by wind, *Hydrol. Process.*, 29(7), 1704–1716, doi:10.1002/hyp.10292, 2015.
- 376 Van Esse, W. R., Perrin, C., Booij, M. J., Augustijn, D. C. M., Fenicia, F., Kavetski, D. and Lobligeois, F.: The
377 influence of conceptual model structure on model performance: A comparative study for 237 French catchments,
378 *Hydrol. Earth Syst. Sci.*, 17(10), 4227–4239, doi:10.5194/hess-17-4227-2013, 2013.
- 379 Ewen, J., Parkin, G. and O’Connell, P. E.: SHETRAN : Distributed River Basin Flow and Transport Modeling
380 System, *J. Hydrol. Eng.*, 5(JULY), 250–258, 2000.
- 381 Freer, J., Beven, K. and Ambrose, B.: Bayesian estimation of uncertainty in runoff prediction and the value of
382 data: An application of the GLUE approach, *Water Resour. Res.*, 32(7), 2161–2173, doi:10.1029/96WR03723,
383 1996.
- 384 Grimaldi, S., Petroselli, A., Alonso, G. and Nardi, F.: Flow time estimation with spatially variable hillslope
385 velocity in ungauged basins, *Adv. Water Resour.*, 33(10), 1216–1223, doi:10.1016/j.advwatres.2010.06.003,
386 2010.
- 387 Grimaldi, S., Petroselli, a. and Nardi, F.: A parsimonious geomorphological unit hydrograph for rainfall–runoff
388 modelling in small ungauged basins, *Hydrol. Sci. J.*, 57(1), 73–83, doi:10.1080/02626667.2011.636045, 2012.



- 389 Guerrero, J. L., Westerberg, I. K., Halldin, S., Lundin, L. C. and Xu, C. Y.: Exploring the hydrological robustness
390 of model-parameter values with alpha shapes, *Water Resour. Res.*, 49(10), 6700–6715, doi:10.1002/wrcr.20533,
391 2013.
- 392 Gupta, V. K. and Waymire, E. D.: On the formulation of an analytical approach to hydrologic response and
393 similarity at the basin scale, *J. Hydrol.*, 65(1-3), 95–123, 1983.
- 394 Gupta, V. K., Waymire, E. and Wang, C. T.: A representation of an instantaneous unit hydrograph from
395 geomorphology, *Water Resour. Res.*, 16(5), 855–862, doi:10.1029/WR016i005p00855, 1980.
- 396 Hipt, F. Op de, Diekkrüger, B., Steup, G., Yira, Y., Hoffmann, T. and Rode, M.: Applying SHETRAN in a
397 Tropical West African Catchment (Dano, Burkina Faso)—Calibration, Validation, Uncertainty Assessment,
398 *Water*, 9(2), 101, 2017.
- 399 Hrachowitz, M., Savenije, H. H. G., Blöschl, G., McDonnell, J. J., Sivapalan, M., Pomeroy, J. W., Arheimer, B.,
400 Blume, T., Clark, M. P., Ehret, U., Fenicia, F., Freer, J. E., Gelfan, a., Gupta, H. V., Hughes, D. a., Hut, R. W.,
401 Montanari, a., Pande, S., Tetzlaff, D., Troch, P. a., Uhlenbrook, S., Wagener, T., Winsemius, H. C., Woods, R. a.,
402 Zehe, E. and Cudennec, C.: A decade of Predictions in Ungauged Basins (PUB)—a review, *Hydrol. Sci. J.*, 58(6),
403 1198–1255, doi:10.1080/02626667.2013.803183, 2013.
- 404 Jain, S. K., Singh, R. D. and Seth, S. M.: Design flood estimation using GIS supported GIUH approach, *Water*
405 *Resour. Manag.*, 14(5), 369–376, doi:10.1023/A:1011147623014, 2000.
- 406 Jain, V. and Sinha, R.: Derivation of unit hydrograph from GIUH analysis for a Himalayan river, *Water Resour.*
407 *Manag.*, 17(5), 355–375, doi:10.1023/A:1025884903120, 2003.
- 408 Kelly, S. F. and Cuenca, R. H.: BOREAS HYD-01 Soil Hydraulic Properties. Data set. Available on-line
409 [<http://www.daac.ornl.gov>] from Oak Ridge National Laboratory Distributed Active Archive Center, Oak Ridge,
410 Tennessee, U.S.A., Tennessee, USA., 1998.
- 411 Kirpich, Z. P.: Time of concentration of small agricultural watersheds, *Civ. Eng.*, 10(6), 362, 1940.
- 412 Kirshen, D. M. and Bras, R. L.: The linear channel and its effect on the geomorphologic IUH, *J. Hydrol.*, 65(1-3),
413 175–208, 1983.
- 414 Kumar, R., Chatterjee, C., Singh, R. D., Lohani, A. K. and Kumar, S.: Runoff estimation for an ungauged
415 catchment using geomorphological instantaneous unit hydrograph (GIUH) models, *Hydrol. Process.*, 21(14),
416 1829–1840, 2007.
- 417 Mockus, V.: Use of storm and watershed characteristics in synthetic hydrograph analysis and application, US
418 Dep. Agric. Soil Conserv. Serv. Latham, MD, 1957.
- 419 Moore, R., Jones, D., Cox, D. and Isham, V.: Design of the HYREX raingauge network, *Hydrol. Earth Syst. Sci.*,
420 4(4), 523–530, doi:10.5194/hess-4-521-2000, 2000.
- 421 Moussa, R.: On morphometric properties of basins, scale effects and hydrological response, *Hydrol. Process.*,
422 17(1), 33–58, doi:10.1002/hyp.1114, 2003.
- 423 Nash, J. E.: The form of the instantaneous unit hydrograph, *Int. Assoc. Sci. Hydrol. Publ.*, 3, 114–121, 1957.
- 424 Nash, J. E. and Sutcliffe, J. V.: River flow forecasting through conceptual models part I—A discussion of
425 principles, *J. Hydrol.*, 10(3), 282–290, 1970.
- 426 Norouzi Banis, Y., Bathurst, J. C. and Walling, D. E.: Use of caesium-137 data to evaluate SHETRAN simulated
427 long-term erosion patterns in arable lands, *Hydrol. Process.*, 18(10), 1795–1809, 2004.



- 428 Parasuraman, K. and Elshorbagy, A.: Toward improving the reliability of hydrologic prediction: Model structure
429 uncertainty and its quantification using ensemble-based genetic programming framework, *Water Resour. Res.*,
430 44(12), 1–12, doi:10.1029/2007WR006451, 2008.
- 431 Parkin, G.: A three-dimensional variably-saturated subsurface modelling system for river basins, Univeristy of
432 Newcastle., 1996.
- 433 Peña, A., Ayuso, J. L. and Giráldez, J. V: Incorporating topologic properties into the geomorphologic
434 instantaneous unit hydrograph, *Phys. Chem. Earth, Part B Hydrol. Ocean. Atmos.*, 24(1-2), 55–58, 1999.
- 435 Pilgrim, D. H.: Isochrones of travel time and distribution of flood storage from a tracer study on a small
436 watershed, *Water Resour. Res.*, 13(3), 587–595, 1977.
- 437 Pilgrim, D. H., Cordery, I. and Baron, B. C.: Effects of catchment size on runoff relationships, *J. Hydrol.*, 58(3-
438 4), 205–221, doi:10.1016/0022-1694(82)90035-X, 1982.
- 439 Rigon, R., Bancheri, M., Formetta, G. and deLavenne, A.: The geomorphological unit hydrograph from a
440 historical-critical perspective, *Earth Surf. Process. Landforms*, 41(1), 27–37, doi:10.1002/esp.3855, 2016.
- 441 Rinaldo, a, Vogel, G. K., Rigon, R. and Rodrigueziturbe, I.: Can One Gauge the Shape of a Basin, *Water Resour.*
442 *Res.*, 31(4), 1119–1127, doi:10.1029/94wr03290, 1995.
- 443 Rinaldo, A. and Rodriguez-iturbe, I.: Geomorphological theory of the hydrological response, *Hydrol. Process.*,
444 10(11), 803–829, doi:10.1002/(SICI)1099-1085(199606)10:6<803::AID-HYP373>3.0.CO;2-N, 1996.
- 445 Rinaldo, A., Marani, A. and Rigon, R.: Geomorphological dispersion, *Water Resour. Res.*, 27(4), 513–525,
446 doi:10.1029/90WR02501, 1991.
- 447 Robinson, J. S., Sivapalan, M. and Snell, J. D.: On the relative roles of hillslope processes, channel routing, and
448 network geomorphology in the hydrologic response of natural catchments, *Water Resour. Res.*, 31(12), 3089–
449 3101, doi:10.1029/95WR01948, 1995.
- 450 Robson, A. and Reed, D.: Flood estimation handbook, Inst. Hydrol. Wallingford, 1999.
- 451 Rodríguez-Iturbe, I. and Valdes, J. B.: The Geomorphologic Structure of Hydrologic Response, *Water Resour. Res.*,
452 15(6), 1409–1420, doi:10.1029/WR015i006p01409, 1979.
- 453 Rodríguez-Iturbe, I., González-Sanabria, M. and Bras, R. L.: A geomorphoclimatic theory of the instantaneous
454 unit hydrograph, *Water Resour. Res.*, 18(4), 877–886, doi:10.1029/WR018i004p00877, 1982.
- 455 Rojas-Serna, C., Lebecherel, L., Perrin, C., Andréassian, V. and Oudin, L.: How should a rainfall-runoff model
456 be parameterized in an almost ungauged catchment? A methodology tested on 609 catchments, *Water Resour.*
457 *Res.*, 52(6), 4765–4784, doi:10.1002/2015WR018549, 2016.
- 458 Sahoo, B., Chatterjee, C., Raghuvanshi, N. S., Singh, R. and Kumar, R.: Flood Estimation by GIUH-Based Clark
459 and Nash Models, *J. Hydrol. Eng.*, 11(6), 515–525, doi:10.1061/(ASCE)1084-0699(2006)11:6(515), 2006.
- 460 Sawicz, K. a., Kelleher, C., Wagener, T., Troch, P., Sivapalan, M. and Carrillo, G.: Characterizing hydrologic
461 change through catchment classification, *Hydrol. Earth Syst. Sci.*, 18(1), 273–285, doi:10.5194/hess-18-273-
462 2014, 2014.
- 463 Sherman, L. K.: Streamflow from rainfall by the unit-graph method, *Eng. News Rec.*, 108, 501–505, 1932.
- 464 Singh, P. K., Mishra, S. K. and Jain, M. K.: A review of the synthetic unit hydrograph: from the empirical UH to
465 advanced geomorphological methods, *Hydrol. Sci. J.*, 59(2), 239–261, doi:10.1080/02626667.2013.870664,
466 2014.



- 467 Singh, V. P.: Hydrologic systems. v. 1. Rainfall-runoff modeling., 1988.
- 468 Sivapalan, M.: Prediction in ungauged basins: a grand challenge for theoretical hydrology, *Hydrol. Process.*,
469 17(15), 3163–3170, doi:10.1002/hyp.5155, 2003.
- 470 Snyder, F. F.: Synthetic unit-graphs, *Eos, Trans. Am. Geophys. Union*, 19(1), 447–454, 1938.
- 471 Taylor, A. B. and Schwarz, H. E.: Unit-hydrograph lag and peak flow related to basin characteristics, *Eos, Trans.*
472 *Am. Geophys. Union*, 33(2), 235–246, 1952.
- 473 Valdés, J. B., Fiallo, Y. and Rodríguez-Iturbe, I.: A rainfall-runoff analysis of the geomorphologic IUH, *Water*
474 *Resour. Res.*, 15(6), 1421–1434, doi:10.1029/WR015i006p01421, 1979.
- 475 Young, A. R.: Stream flow simulation within UK ungauged catchments using a daily rainfall-runoff model, *J.*
476 *Hydrol.*, 320(1), 155–172, 2006.
- 477 Younger, P. M., Freer, J. E. and Beven, K. J.: Detecting the effects of spatial variability of rainfall on
478 hydrological modelling within an uncertainty analysis framework, *Hydrol. Process.*, 23, 1988–2003,
479 doi:10.1002/hyp, 2009.
- 480 Zhang, R., Santos, C. A. G., Moreira, M., Freire, P. K. M. M. and Corte-Real, J.: Automatic calibration of the
481 SHETRAN hydrological modelling system using MSCE, *Water Resour. Manag.*, 27(11), 4053–4068, 2013.
- 482 Zhuo, L., Dai, Q. and Han, D.: Meta-analysis of flow modeling performances-to build a matching system
483 between catchment complexity and model types, *Hydrol. Process.*, 29(11), 2463–2477, doi:10.1002/hyp.10371,
484 2015.
- 485



Processes	Equation
Subsurface flow	Variably saturated flow equation (3D) (Parkin, 1996)
Overland flow	Saint-Venant equations, diffusion approximation (2D) (Abbott et al., 1986)
Channel flow	Saint-Venant equations, diffusion approximation (flow in a network of 1D channels)
Canopy interception and drip	Rutter equation (Abbott et al., 1986)
Evaporation	Penman-Monteith equation (or as fraction of potential evaporation rate) (Abbott et al., 1986)
Snowpack and melt*	Accumulation equation and energy budget melt equation (or degree-day melt equation) (Abbott et al., 1986)

486 * Snowpack and melt is not considered in this study.

487

488 **Table 1.** Equations of hydrological processes in SHETRAN



		$Tp = aL^b$					
Storm*	Slope (m km-1)	a_2	b_2	Slope (m km-1)	Storm*	a_3	b_3
	14.59	0.94	1.07		10×1	0.59	1.14
	17.51	0.86	1.08		20×1	0.54	1.04
	20.43	0.79	1.09		30×1	0.53	0.98
	23.34	0.72	1.10		50×1	0.38	0.99
	26.26	0.64	1.12		60×1	0.38	0.97
	29.18	0.59	1.13		80×1	0.49	0.88
10×1	58.36	0.56	1.11	29.18	100×1	0.60	0.92
	87.54	0.54	1.09		200×1	2.76	0.58
	116.72	0.53	1.07		10×2	0.66	1.00
	Catchment shape	a_4	b_4		10×5	1.07	0.78
	A	0.59	1.14		10×10	2.51	0.83
	B	0.44	1.23		10×15	5.46	0.47
	C	0.63	1.17		10×20	10.03	0.35

489 *Storm is presented by rainfall intensity (mm h⁻¹) × duration (h)

490

491 **Table 2.** The coefficients of equations of Tp and drainage length



	Area (km ²)	Drainage length (km)	Slope (m km ⁻¹)
A	137	12.12	29.18
B	142	12.35	29.18
C	140	16.97	29.18

492

493 **Table 3.** The catchment properties of the three cloned catchments

494



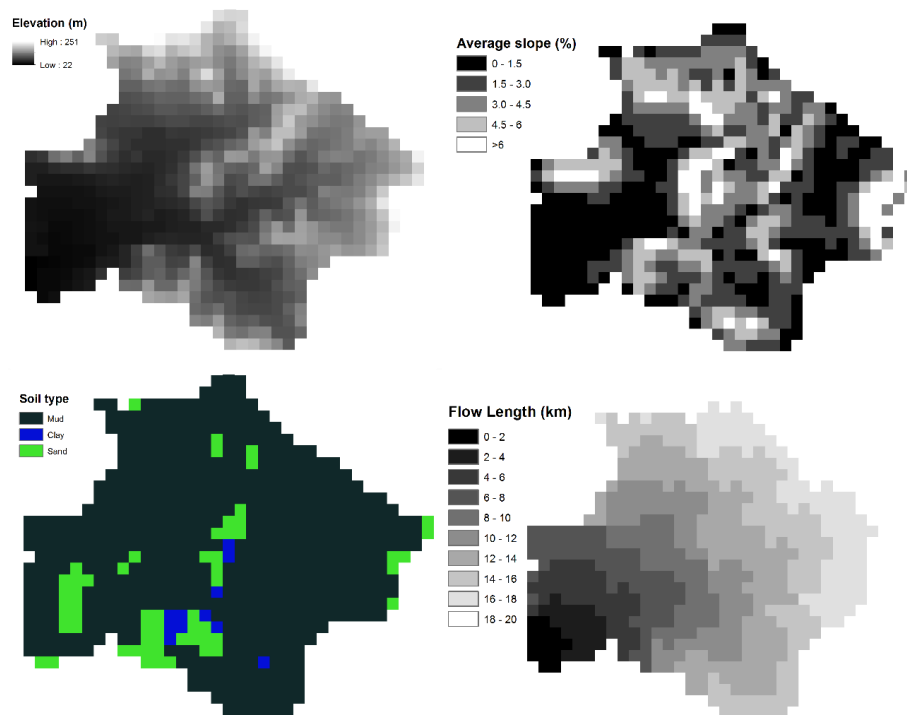
Storm*	$Qp = aL^b$			$Qp = \frac{c}{Tp}$			
	Slope (m km ⁻¹)	a_5	b_5	c	Slope(m km ⁻¹)	Storm*	c
	14.59	0.45	-0.86	0.74		10×1	3.21
	17.51	0.57	-0.94	0.79		20×1	3.86
	20.43	0.59	-0.94	0.81		30×1	3.99
	23.34	0.61	-0.94	0.83		50×1	4.31
	26.26	0.64	-0.94	0.83		60×1	4.83
	29.18	0.65	-0.93	0.8		80×1	5.22
10×1	58.36	0.82	-0.95	0.88	29.18	10×10	7.56
	87.54	0.94	-0.96	0.92		10×20	9.04
	116.72	0.98	-0.94	0.9		100×1	5.82
	Catchment shape	a_5	b_5	c		200×1	5.49
	A	0.65	-0.93	0.8		10×2	3.68
	B	0.67	-0.98	0.8		10×5	5.93
	C	0.99	-1.03	0.99		10×15	8.49

495 *Storm is presented by rainfall intensity (mm h⁻¹) × duration (h)

496

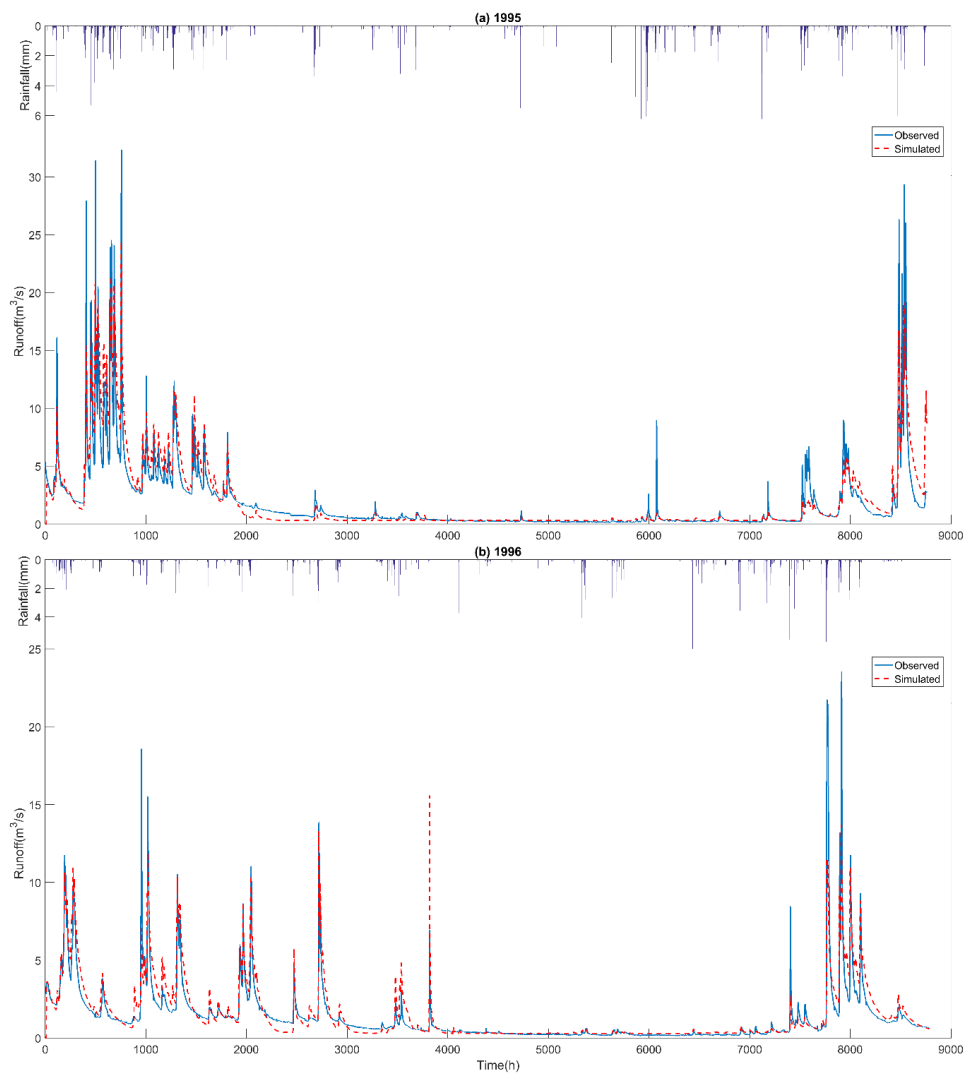
497 **Table 4. The coefficients in equations of Qp**

498



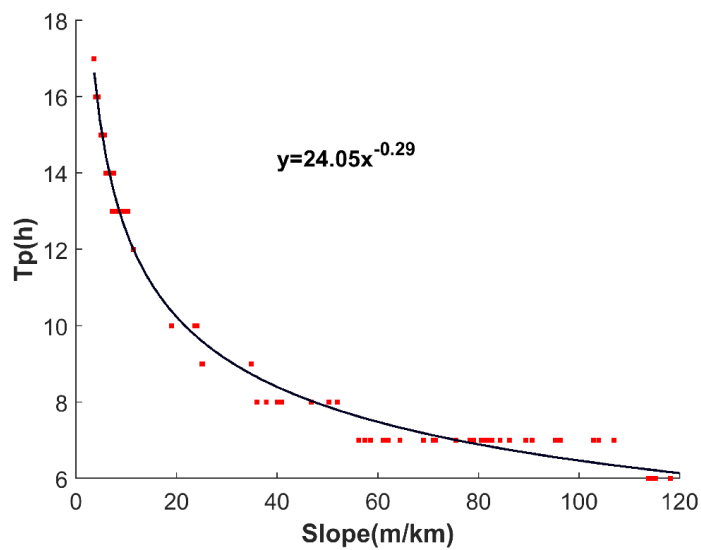
499

500 **Figure 1. Spatial data for the baseline model of the Brue catchment (500m grid)**



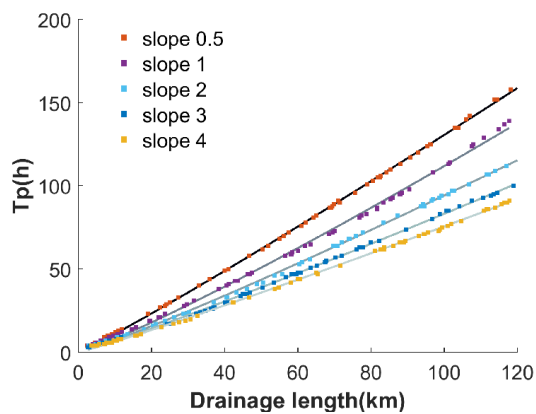
501

502 **Figure 2. Hydrographs of the model calibration and validation**



503

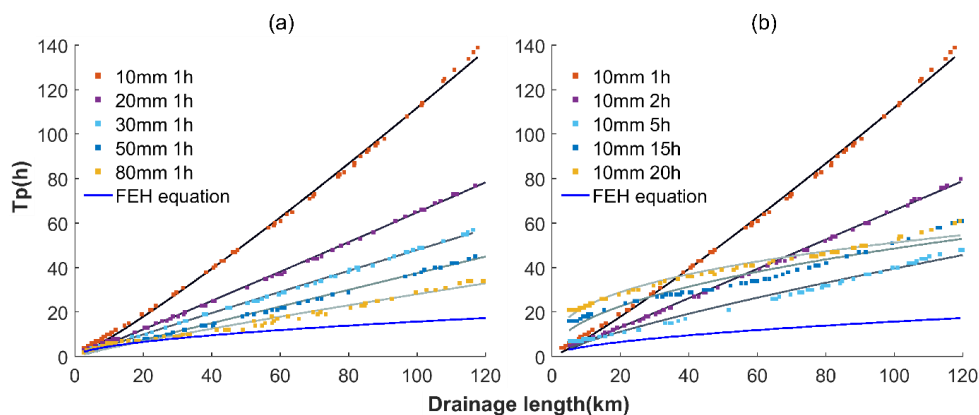
504 **Figure 3. The relationship between Tp and the average slope**



505

506

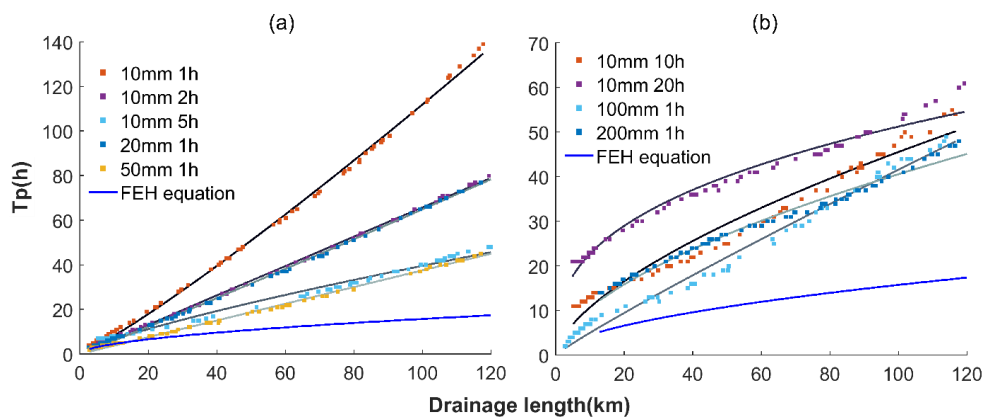
Figure 4. The relationship between T_p and the drainage length with different slopes



507

508

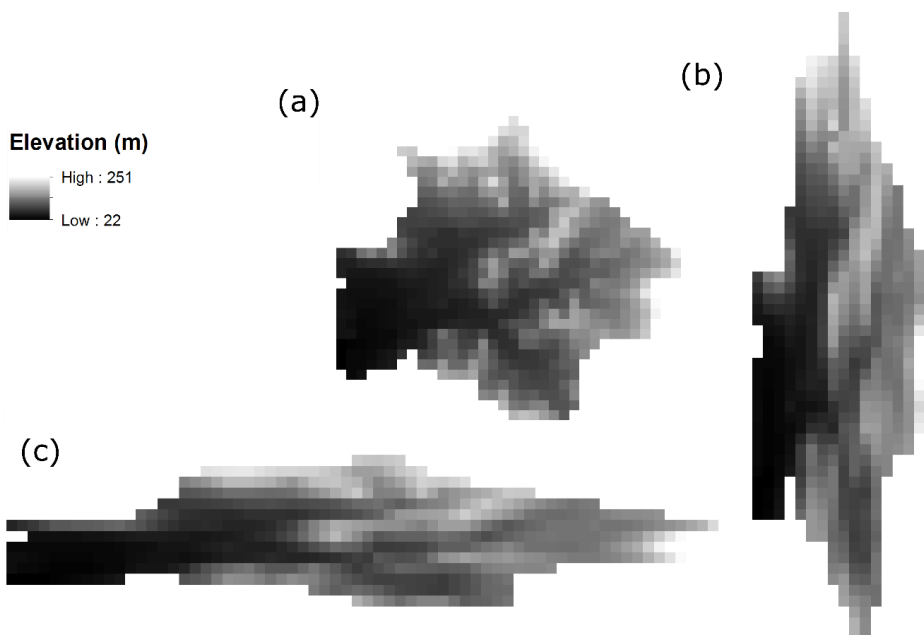
Figure 5. The relationship between T_p and drainage length in different storms



509

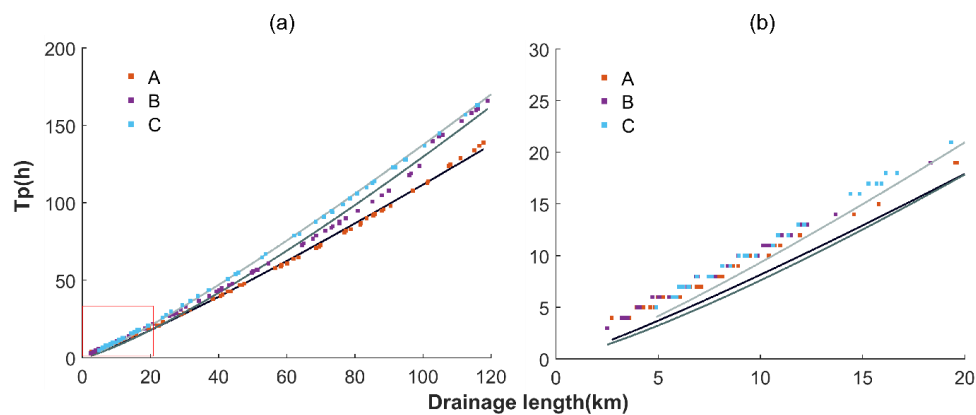
510

Figure 6. The relationship between T_p and the drainage length in different storm patterns



511

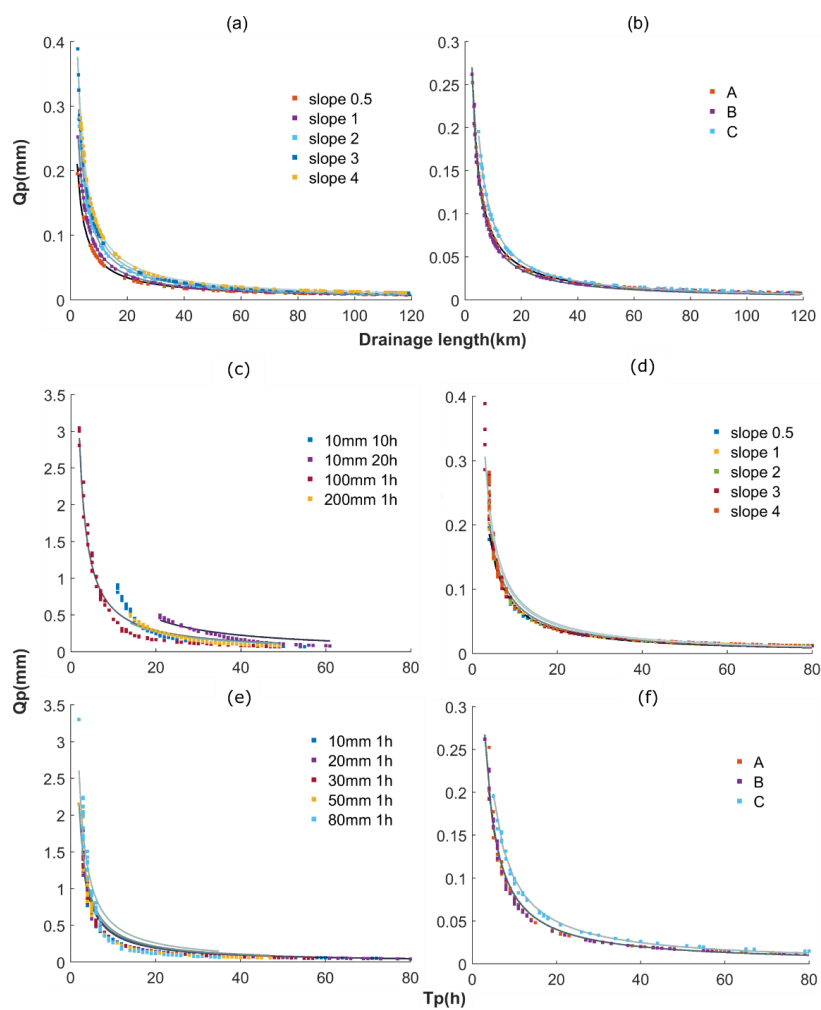
512 **Figure 7. Three catchments with different shapes**



513

514

Figure 8. The relationship between T_p and drainage Length in three catchments with different shapes



515

516 **Figure 9. The relationship between Q_p and Drainage length (a)-(b), Q_p and T_p (c)-(f) in different slopes and shapes**

517